Analysis and Segmentation of the Bone Cancer MRI Image Based On Neural Networks Approach Model

Dr.K.Baskaran[1], Dr.R.Malathi[2]

[1]Associate Professor/ECE Aditya College of Engineering, Madanapalle, Andhra Pradesh, India.
[2]Professor/EIE Annamalai University Chidambaram, Tamil Nadu, India
Corresponding Author: Dr.K.Baskaran

Abstract - *The manual segmentation of the Magnetic Resonance Imaging (MRI) bone image presents the following two issues: 1) it is tedious and time demanding task that can be only performed by a specialized clinician; and 2) it is prone to poor repeatability. These issues can be solve with the use of automatic bone image segmentation system, which has the potential to improve work flow in a in a clinical site and decrease the variability between user segmentations. This paper deals with segmentation of bone magnetic resonance imaging images based on semi supervised and dynamic model. The prime objective is to delineate the outline of an irregularity in an MRI image of the bone. Accurate and robust segmentation of bone tissue many employ applications such as surgery and radio therapy. It has been successful in segmenting the bone in every images acquired from several different MRI scanners, using different ego sequences. By using semi supervised method used to reduce the dependence on a rich initial training set and dynamic model to decrease the search complexity. The performance of and approach is calculated using a data set of diseased cases containing 100 annotated images and another data set of normal cases containing 20 annotated images. Further these techniques are also used to find irregularities in lung images.*

Index Terms - *segmentation, region merging, region of interest, magnetic resonance imaging, Transduction and Inferences.*

I.   Introduction

Segmentation is an image processing operation which aims to partition an image into homogeneous regions composed of pixels with the same characteristics according to predefined criteria. Most methods of image segmentation requires the adjustment of several control parameters to obtain good results but the multi sensor scales canny requires no fitting parameters.

Bone Sarcoma is relatively uncommon, accounting for 0.5% to 1% of malignant neoplasms. Various causative agents, including exposure to ionizing radiation, have been associated with the development of bone sarcoma the development of bone sarcoma in adults and children following therapeutic or occupational exposure to high-dose ionizing radiation [9]. Other studies have also demonstrated an association between exposure to relatively high levels of internal sources of radiation and the development of an excess of bone sarcomas. Additional information of interest regarding the bone sarcoma cases included sex, city of exposure, age at the time of the bombing, age at diagnosis, time from exposure to diagnosis, survival period, and survival status at the time of the latest follow-up, and cause of death. Furthermore, a review of the clinical records was also conducted to determine the exact tumor location, the treatment type, the presence of metastatic disease, and any other relevant clinical characteristics. In addition, the bone marrow dose (in grays) was estimated, with the neutron dose given a weight of 10 and the gamma radiation dose given a weight of 1 to adjust for biological effectiveness

The data consist of healthy brain and a bone with a tumour.
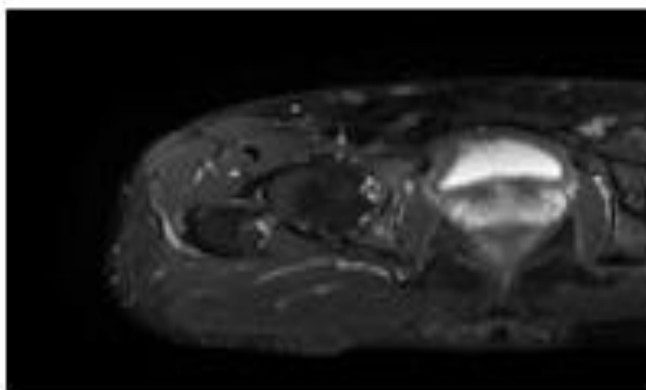
Fig. 1. MRI Image of the bone with tumour
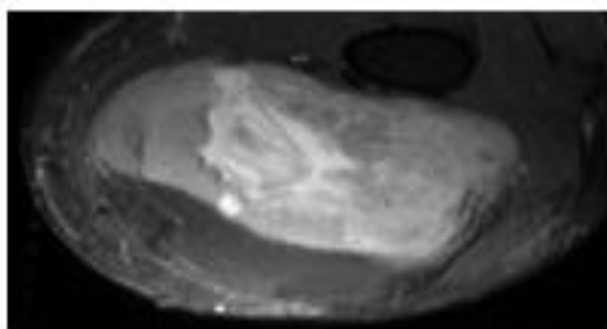
Fig. 2. MRI image of the other parts bones from a tumour.

It provides detailed images of living tissues, and is used for both bone and body human studies. Data obtained from MR images is used for detecting tissue deformities such as cancers and injuries; MR is also used extensively in studies of brain pathology, where regions of interest (ROI's) are often examined in detail, for example in multiple sclerosis (MS) studies [16]. In order to perform good quantitative studies, ROI's within the brain must be well defined. In traditional methods, a skilled operator manually outlines the ROI's using a mouse or cursor. More recently, computer-assisted methods have been used for specific tasks such as extraction of MS lesions from MRI brain scans [14], or extraction of the cerebral ventricles in schizophrenia studies [15]. Many of these computer-assisted tasks require segmentation of the whole brain from the head, either because the whole brain *is* the ROI such as in Alzheimer's studies [18] or because automatic ROI extraction using statistical methods is made easier if the skull and scalp have been removed [13].

We describe our automatic method for segmenting the brain from the head in MR images. The key to any automatic method is that it must be robust, so that it produces reliable results on every image acquired from any MR scanner using different relaxation times, slice thicknesses and fields of view. Our method is so robust, that it successfully was able to segment the brain in every slice of 40 head images from five different MRI scanners (all 1.5-T; four from GE, one from Siemens), using several different spin-echo images with different echo times, and with two T1-weighted gradient pulse sequences. Our method works in the presence of typical radio frequency (RF) in homogeneity and it addresses the partial volume effect in a consistent reasonable manner. The method is partly two-dimensional (2-D)-based and partly three-dimensional (3-D)-based, and it works best on routine axially displayed multispectral dual-echo proton density (PD) and T2 (spin-spin relaxation time) sequences. It also works well on axial and coronal 3-D T1-weighted SPGR (Spoiled Gradient) sequences.

However, it does *not* work fully automatically on sagittal displayed 3-D T1-weighted images where accurate localization of cortical convolutions is required, as parameter tuning is necessary to include the thin dark brain areas and keep the cerebellum attached to the rest of the brain, while simultaneously separating the brain from the back of the neck tissue and the cheeks. For such sagittal displayed images, other techniques such as those described in [1] and [24] are available.

II. Training Procedure

For the rigid classifier, we follow the multi scale implementation in [12] and build an image scale space produced from the convolution of the Gaussian kernel with the input image , as follows: (7) where is the scale parameter, is the image coordinate, is the convolution operator, and Assuming that our multi scale implementation uses a set of image.

$$L(X,\sigma)=G(X,\sigma)*I(X) \tag{1}$$

Where σ is the scale parameter is the image coordinate, * is the convolution operator, and

$$G(X,\sigma) = \frac{1}{2\pi\sigma^2}\exp\frac{(X-\mu)}{2\sigma} \tag{2}$$

The sets of positives and negatives are formed by sampling the distribution over the training rigid parameters, which can be defined as

$$Dist(D) = \begin{cases} u(r(\Theta)), & \text{if uniform distribution is assumed} \\ G(\mu,\sum & \text{if normal distribution is assumed} \end{cases}$$

(3)

Classification assigns images or instances or examples to one of the predefined classes and is a determined problem encompassing in variety of applications. The classification helps to categorize images as malignant or benign based on MRI scan, detect fractures, tumors and classifying tumors based on shapes. The classifier algorithm enhances datasets performances. To build or train a classifier creates a function or data structure that determines the class attribute's missing value of the new unclassified instances [1]

Classification is a data mining machine/learning technique which predicts group class for data instances. It detects data classes aided by known classes learnt during training. This kind of learning is called supervised classification. Soit places new instances in different classes based on the quantitative data obtained from one or more measurements, qualities or features, and based on training set where predefined classes are established beforehand. But, classification where no expert is present to predict is called unsupervised classification. A model is defined where attributes set define classes. Various classifiers and algorithms exist.[2]

III. Semi Supervised Leering

In this work, we examine an approach to solve classification problems that combines supervised and unsupervised learning techniques. In supervised learning, we assume we are given a set of labelled training points, and the task is to construct some function that will correctly predict the labels of future points. In unsupervised learning such as clustering, the task is to segment unlabeled training data into clusters that reflect some meaningful structure in the data. For the Semi-Supervised Learning Problem (SSLP) we assume that we are given both labelled and unlabeled points. The task is then to predict the labels of the [4] unlabeled points using all the available labelled data, as well as unlabeled data. One would expect a better generalization ability of the resulting classifier due to the better understanding of the input distribution resulting from using all the available data. The semi-supervised learning problem [6] can be used to perform transductive inference. In transduction, we are given a set of training data and a set of testing data, and the learning task is to predict the labels of the specific testing data only. Different testing data will produce different classification functions. The intuition is that transduction is a simpler problem because we are trying to construct a function that is valid only at specific points, versus in induction where the goal is to construct a function valid at all future testing points.

As a base to our semi-supervised algorithm, we use an unsupervised clustering method optimized with a genetic algorithm incorporating a measure of classification accuracy used in decision tree algorithms, the GINI index . Here we examine clustering algorithms that minimize some objective function applied to k-cluster centres. Each point is assigned to the nearest cluster centre by Euclidean distance. The goal is to choose the cluster centres that minimize some measure of cluster quality. Typically a cluster dispersion metric is used. If the mean square error, a measure of within cluster variance, is used than the problem becomes similar to the classic K-means clustering.

A common objective function in these implementations is to minimize the square error of the cluster dispersion:

$$E = \sum_{K-1X\epsilon C_K}^{K}\sum || X - M_J ||^2 \tag{4}$$

Where K is the number of clusters, mk is the centre of cluster Ck. This is indeed the objective function for the K-means clustering algorithms.

IV. Semi Supervised Learning Algorithm

• Within genetic algorithm:
1. Determine cluster centres
2. Partition the labelled data by distance to closest cluster centre.
3. Find non-empty clusters, assign a label to non-empty clusters by majority class vote within them.
4. Compute dispersion and impurity measures:
− Induction: Use labelled data.
− Transduction: Use labelled + unlabeled data.
• Prune clusters with few members.
• Reassign the points to final non-empty clusters

FIRST DISPERSION MEASURE: MSE

The average within cluster variance is frequently used in clustering techniques as a measure of cluster quality.

Commonly known as the mean square error (MSE), this quantity is defined as:

$$E = \frac{1}{N} \sum_{K-1 \varepsilon C_K}^{K} \| X - M \|^2 S \qquad (5)$$ where N is the

number of points, K is the number of clusters, and mk is the centre of cluster Ck. The K-means algorithm minimizes the MSE objective.

If mj and mk are the centres of Cj and Ck, then and Djk = kmj − mkk2, where mj is the centre of cluster Cj consisting of Nj points.

Clustering algorithms are widely used in pattern recognition. Now the DBI is defined as:

$$(6)E = \frac{1}{N_J} \sum_{K-1 X \varepsilon C_K}^{K} \sum \| X - M_J \|^2$$

$$E = \| X - M_J \|^2 \qquad (7)$$

V. Impurity Measure: Gina-Index

The Gini index has been used extensively in the literature to determine the impurity of a certain split in decision trees. Usually, the root and intermediate nodes are partitioned to two children nodes. In this case, left and right nodes will have different Gini index values.

In this case, Gini Index of a certain cluster is computed as:

$$R = \max_{j \neq k} R_{J,K} \qquad (8)$$

where Pji is the number of points belong to ith class in cluster j. Nj is the total number of points in cluster j. The impurity measure of a particular partitioning into K clusters is: impurity = PK

$$DB(K) = \frac{1}{K} \sum_{K=1}^{K} R_K \qquad (9)$$

where N is the number of points in the dataset.

VI. Experimental Result

The goals in this computational approach are to determine if combining supervised and unsupervised learning approaches techniques could lead to improved generalization, and to investigate if performing transductive inference using un-labelled data for training could lead to improvements over inductive inference [9].

For transduction, both the cluster dispersion measure and the Gini index are based on the labelled and unlabeled data.

In transduction, the Gini index becomes:

$$GiniP_J = 1.0 - \sum_{t=1}^{K} (\frac{P_{ji}}{Nji})^2 \; j \text{ in } k,1...k \qquad (10)$$

j is equal to number of labelled and unlabeled points in cluster j. The best parameter set for the problem was picked by trial and error. We use same set of GA parameters for each dataset.

VII. Dynamic Programming

Boundary definition via dynamic programming can be formulated as a graph searching problem where the goal is to find the optimal path between a set of start nodes and a set of end nodes. Typical applications of the use of dynamic programming in boundary tracking problems are tracing borders of elongated objects like roads and rivers in aerial photographs and the segmentation of handwritten characters. Medical applications include the segmentation of spine boundaries and tracing vessel borders. To apply dynamic programming to find the boundary of a mass we notice that the shape of most masses is approximately circular. This circularity constraint is implemented by carrying out the calculations in polar space. For the transform we use a circular region of interest (ROI) with centre (x; y) and radius R. The center of the ROI defines the origin for the coordinate transform and should be within the suspect lesion.

VIII. Local Cost

Local cost is cost assigned to each pixel in the polar image. This cost should embody a notion of a good boundary: pixels that possess many characteristics of the searched boundary are assigned low cost and vice versa. The local cost components form the following cost function:

$$c(i, j) = w_s s(i, j) + w_d d(i, j) + w_g g(i, j) \tag{11}$$

where s represents the edge strength, d the deviation from an expected size, and g the deviation from an expected gray level. The weights for the components are given by ws, wd and wg.

A. Edge Strength s(i; j) As most contours exhibit strong edges we want to assign pixels with strong edge features low cost. The edge strength for each pixel is determined by calculating the gradient magnitude in the direction normal to the contour. This corresponds with the gradient in vertical direction in the polar image [28].Then the relative edge strength is determined by normalizing the gradient values with the maximum gradient max(y0). This normalization ensures that subtle contours with low global but high local edge strength can be found as well. The normalized gradient value is inverted so high gradients produce low costs and vice versa. The gradient component function is

$$s(i, j) = \frac{\max(y') - y'(i, j)}{\max} \tag{12}$$

where y0 is the gradient magnitude in vertical direction. For max(y0) we took the [99th] percentile of the gradient values measured in the ROI. By taking the 99th percentile it is prevented that one outlier, for instance a very bright micro-calculation, decreases the relative edge strength of all other pixels in the ROI.

B. Mass size d(i; j) Contours that enclose a mass with a size common for masses are assigned low cost value. On the other hand, very small and very large segmentations are assigned higher cost. Most masses have a radius between 5 mm and 15 mm, with a mean radius of about 9 mm [13]. The following formula was used to incorporate size information in the cost function:

$$d(i, j) = \begin{cases} (j, \mu)^2 & : j \le m \\ (m, \mu)^2 & : j \ge m \end{cases} \tag{13}$$

where is the mean radius of masses. A cost limit m is set to prevent that the size component of the cost function completely determines the value of the cost function for large masses. This limit is set to 15 mm. alternatively; the cost component for mass size could be obtained by estimating the size distribution of masses. The probabilities for each size could then be used to determine the cost value d(i; j). To use this method a large representative database with benign and malignant masses of known size is needed to accurately determine the probabilities for each mass size. Currently we used the method as we do not have an independent database that we can use for this purpose.

C. Deviation from expected gray level g(i; j) Another characteristic of the mass boundary is the gray level. This gray level should correspond with the edge of the object. A common assumption is that this edge is located at the zero crossing of the second derivative of the edge profile. In projective images however, the real edge is located toward the darker side (background). Consequently, the gray value of the border will have a value close to the background gray level [14]. By estimating the intensity distribution of the mass and the background a preferred gray level for the contour can be determined.

$$g = \alpha \mu_{\max} + (1 - \alpha) \mu_{background} \tag{14}$$

where α should be smaller than 1/2 to ensure the edge is located more toward the background level. The gray level component of the cost function is defined as

$$g(i, j) = sqrt(abs(G(i, j) - g) \qquad (15)$$

where G(i; j) is the intensity value of the pixel (i; j).

D. Dynamic programming shortest path finding algorithm

Application of the cost function to all pixels in the polar image results in the so called cost image. This image can be seen as a graph in which the dynamic programming algorithm should 2nd the path with the lowest cost. The 1rst column in the cost image c(i; 0) represents the start nodes for the algorithm, whereas the end nodes are represented by the pixels in the last column of the image[32]. The cumulative cost of each path is stored in the cumulative cost matrix. The cumulative cost matrix is constructed in two steps. First the cumulative costs of pixels in the 1rst column are set equal to the cost of these pixels:

$$C(i,0) = c(i,0) \qquad (16)$$

where C(i; j) is the cumulative cost and c(i; j) is the cost value for pixel (i; j) in the polar image. For the other pixels the cumulative cost is calculated by a recursive step:

$$c(i, j+1) = \min_{-m \le l \le m} ((i+1, j) + (i, j+1) + h(l) \quad (17)$$

The additional cost of a segment of the path for column j to j+1 depends on the cost value of pixel (i; j) and the direction l. The cost of the direction is set according to a function h(l) which we use to control smoothness. h(l) is set to zero for directions outside the interval . The final contour is found by selecting those pixels that linked together from the boundary with the lowest cost. The endpoint C (i;j) of the contour is the pixel in the last column of the cumulative cost matrix with the lowest cost.

IX. Training and Testing Data Set

A NN model must be trained with representative data before use. Two training types are supervised and unsupervised. The idea behind training is to pick up set of weights (often randomly), apply inputs to NN and check output with assigned weights. The computed result is then compared to actual value. The difference updates weights of each layer using a generalized delta rule. This training algorithm is called back propagation. NN is considered trained when after many training epochs, error between actual output and computed output is less than a specified value, The NN when trained processes new data, classifying them according to required knowledge.

When using supervised training it is important to address the listed below practical issues [25] when using supervised training.

Over training: This is a serious issue where NN reduces error so that it simply memorizes data set used in training. Then it is impossible to categorize new data set and generalization becomes impossible.

Validation set: Dataset validation is done to prevent over-training. The training precedes straining error decreases and the result of validation set application improves.

Test data: a separate dataset to test trained NN to determine whether it has generalized training data set accurately.

Data preparation: used to scale data before training and improve training process.
A network structure is defined with fixed inputs, hidden nodes and outputs. Second, an algorithm realizes the learning process. But a fixed structure lacks optimal performance in a training period. A small network may not ensure performance due to limited information processing Power. On the other hand a large network may have redundant connections. Cost implementation for a large network is high. Constructive and destructive algorithms are used to obtain network structure automatically. In terms of running time, using a non optimized MATLAB Implementation the full search takes around 20 s to run and gradient
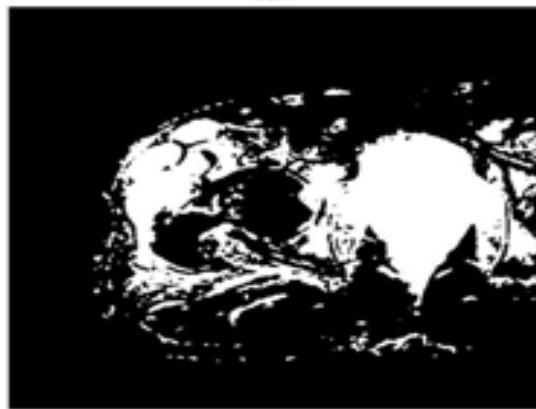
Fig. 3. Segmented Image Region by semi supervised method.
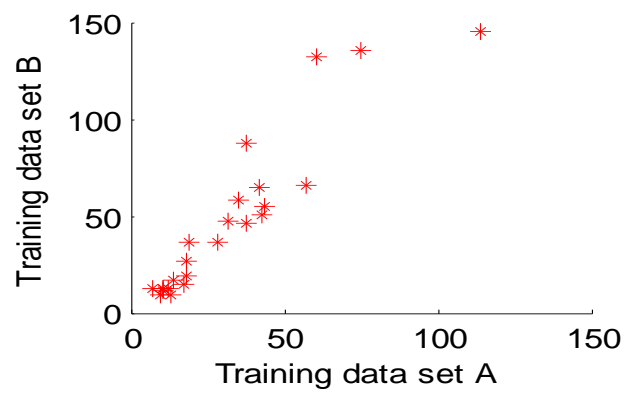
Fig. 4. Scatter plot of two training sequences.ROC curve of train image on sequences T_1, A and T_2, B.
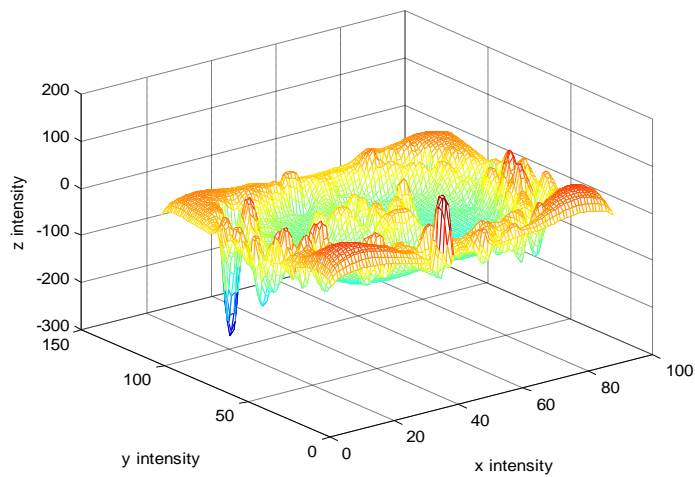
Fig. 5 Contour Plot of Segmented Image.
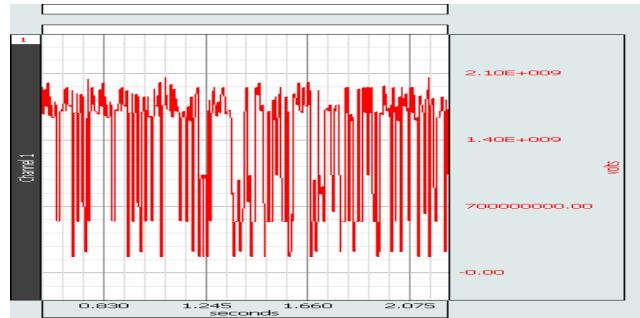
Fig. 6 Normal values not affected Bone Cancer
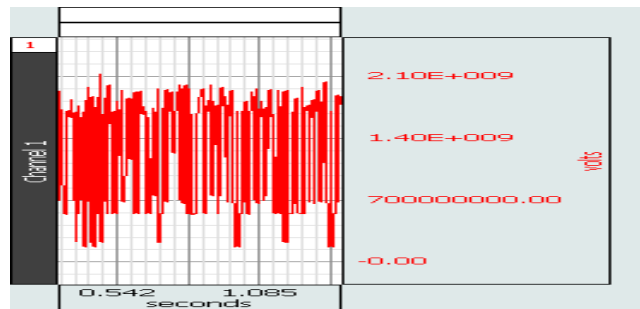
Fig. 6 Abnormal values affected the Bone Cancer
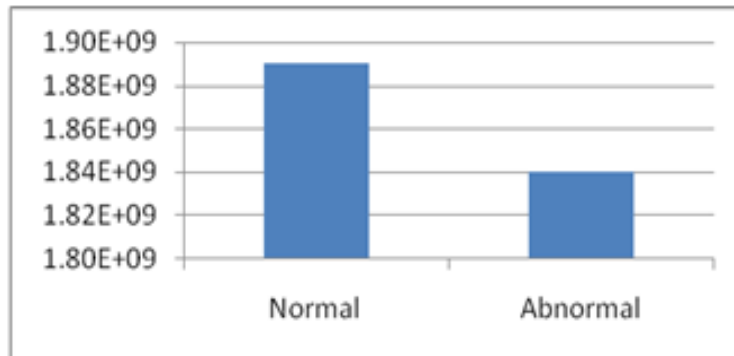
Fig.7 Compare the Peak signal for Normal and Abnormal
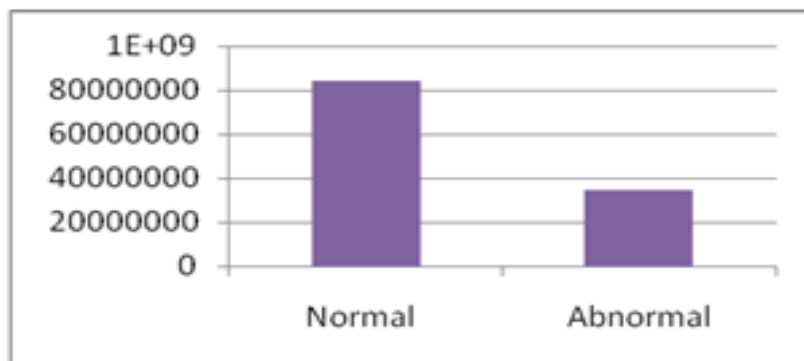
Fig.8 Compare the Area signal for Normal and Abnormal
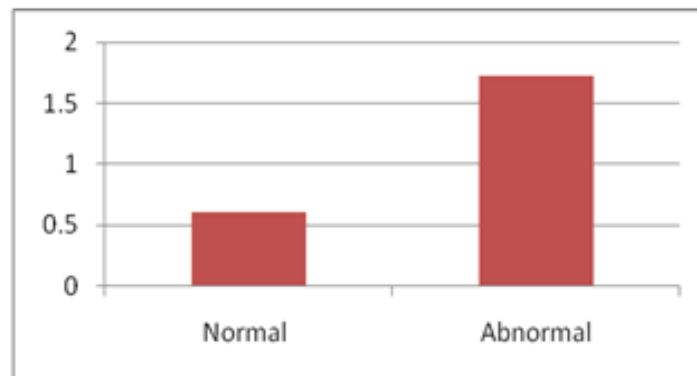
Fig.9 Compare the frequency for Normal and Abnormal

Table 1 Summary NN Model with Semi Supervised Model

Techniques Used / Parameters	NN Model with Semi supervised
Classification of Peak Normal	1.89E+09
Classification of Peak Abnormal	1.84E+09
Classification of Area Normal	8.4E+08
Classification of Area Abnormal	3.47E+08
F(Frequency) measure for Normal	0.602
F(Frequency)measure for Abnormal	1.724

X. Conclusion and Future Work

A novel method for semi-supervised learning that combines supervised and un-supervised learning techniques has been introduced in this paper. The basic idea is to take an unsupervised clustering method, label each cluster with class membership, and simultaneously optimize the misclassification error of the resulting clusters. The intuition behind the approach is that the unsupervised component of objective acts likes a form of regularization or capacity control during supervised learning to avoid over fitting. The objective function is a linear combination of a measure of cluster dispersion and a measure of cluster impurity. The method can exploit any available unlabeled data during training since the cluster dispersion measure does not require class labels. This allows the approach to be used for transductive inference, the process of constructing a classifier using both the labelled training data and the unlabeled testing data. Experimental results also show that using DBI for cluster dispersion instead of MSE helps transductive inference. This is due to the compact and well separated clusters found by minimizing DBI. DBI finds solution using much fewer clusters than MSE with much greater accuracy. Dynamic programming algorithm is used to find the shortest distance pixel for segmenting the image. We also plan to work on a shape model that is less dependent on the training set, similar to the DBN used for the appearance model. Moreover, we plan to apply this approach to other anatomies and other medical imaging techniques.

References

[1].   Bhatia, M., and Gharge, S. (2015), "Segmentation of brain MR image using fuzzy local Gaussian mixture model," In IEEE Electrical Insulation Conference (EIC), pp. 1-5.
[2].   Frighetto-Pereira, L., Metzner, G.A., Azevedo-Marques, P.M., Nogueira-Barbosa, M.H., Oloumi, F., and Rangayyan, R.M. (2016), "Recognition of vertebral compression fractures in magnetic resonance images using statistics of height and width," In IEEE International Symposium on Medical Measurements and Applications (MeMeA), pp. 1-5.
[3].   T. Arden and J. Poon, WiT User's Guide. Logical Vision Ltd., Burnaby, Canada, Oct. 1993, Version 4.1.
[4].   M. S. Atkins and B. Mackiewich, "Automatic segmentation of the brain in MRI," in Proc. Visualization in Biomedical Computing'96,Sept. 1996, vol. 1131, pp. 210–216.
[5].   M. S. Atkins, T. Zuk, B. Johnston, and T. Arden, "Role of visual languages in developing image analysis algorithms," in Proc. IEEE Conf. Visual Languages, St. Louis, MO, Oct. 1994, pp. 262–269.
[6].   C. I. Attwood, G. D. Sullivan, and K. D. Baker, "Recognizing cortical sulci and gyri in MR images," in Proc. British Machine Vision Conf., P. Mowforth, Ed., 1991.
[7].   J. C. Bezdek, L. O. Hall, and L. P. Clarke, "Review of MR image segmentation techniques using pattern recognition," Med. Phys., vol. 20, no. 4, pp. 1033–1048, 1993.

[8]. M. E. Brummer, R. M. Mersereau, R. L. Eisner, and R. R. J. Lewine, "Automatic detection of brain contours in MRI data sets," IEEE Trans. Med. Imag., vol. 12, pp. 153–166, June 1993.

[9]. Baskaran K, Malathi R and Thirusakthimurugan P (2014), The Automatic Segmentation of the Brain MRI Image Using Semi Supervised Approach and Dynamic Model, International Journal of Science and Innovative Engineering & Technology, Communication & Electronics Engineering,Vol. 5, no.8, pp.76.

[10]. A. Chakraborty, L. H. Staib, and J. S. Duncan, "An integrated approach to boundary finding in medical images," in Proc. IEEE Workshop on Biomedical Image Analysis, Los Alamos, CA, June 1994, pp. 13–22.

[11]. V. Chalana, W. Costa, and Y. Kim, "Integrating region growing and edge detection using regularization," in Proc. SPIE Conf. Medical Imaging, 1995.

[12]. L. P. Clarke, R. P. Velthuizen, M. A. Camacho, J. J. Heine, M. Vaidyanathan, L. O. Hall, R. W. Thatcher, and M. L. Silbiger, "MRI segmentation: Methods and applications," Magn. Reson. Imag., vol. 13, no. 3, pp. 343–368, 1995.

[13]. H. E. Cline, W. E. Lorensen, R. Kikinis, and F. Jolesz, "Threedimensional segmentation of MR images of the head using probability and connectivity," J. Comput. Assist. Tomogr., vol. 14, no. 6, pp. 1037–1045, Nov./Dec. 1990.

[14]. D. L. Collins, G. Le Goualher, R. Venugopal, A. Caramanos, A. C. Evans, and C. Barillot, "Cortical constraints for nonlinear cortical registration," in Proc. Visualization in Biomedical Computing'96, Sept. 1996, vol. 1131, pp. 307–316.

[15]. C. A. Davatzikos and J. L. Prince, "An active contour model for mapping the cortex," IEEE Trans. Med. Imag., vol. 14, pp. 65–80, Mar. 1995.

[16]. D. Dean, P. Buckley, F. Bookstein, J. Kamath, D. Kwon, L. Friedman, and C. Lys, "Three dimensional MR-based morphometric comparison of schizophrenic and normal cerebral ventricles," in Proc. Visualization in Biomedical Computing'96, Sept. 1996, vol. 1131, pp. 363–372.

[17]. P. Van den Elsen, J. B. A. Maintz, E.-J. D. Pol, and M. Viergever, "Automatic registration of CT and MR brain images using correlation of geometrical features," IEEE Trans. Med. Imag., vol. 14, pp. 384–395, June 1995.

[18]. W. A. Edelstein, P. A. Bottomley, and L. M. Pfeifer, "A signal-to-noise calibration procedure for NMR imaging systems," Med. Phys., vol. 11, no. 2, pp. 180–185, 1984.

[19]. P. A. Freeborough and N. C. Fox, "Assessing patterns and rates of brain atrophy by serial MRI: A segmentation, registration, display and quantification procedure," in Proc. Visualization in Biomedical Computing'96, Sept. 1996, vol. 1131, pp. 419–428.

[20]. Y. Ge, J. M. Fitzpatrick, B. Dawant, J. Bao, R. Kessler, and R. Margolin, "Accurate localization of cortical convolutions in MR brain images," IEEE Trans. Med. Imag., vol. 15, pp. 418–428, Aug. 1996.

[21]. G. Gerig, O. K̈ubler, R. Kikinis, and F. A. Jolesz, "Nonlinear anisotropic filtering of MRI data," IEEE Trans. Med. Imag., vol. 11, no. 2, pp. 221–232, June 1992.

[22]. Henkelman, "Measurement of signal intensities in the presence of noise in MR images," Med. Phys., vol. 12, no. 2, pp. 232–233, 1985.

[23]. B. Johnston, M. S. Atkins, and K. S. Booth, "Partial volume segmentation in 3-D of lesions and tissues in magnetic resonance images," in Proc. SPIE-Medical Imaging 1994, Bellingham, WA, 1994, vol. 2167, pp. 28–39,

[24]. B. Johnston, M. S. Atkins, B. Mackiewich, and M. Anderson, "Segmentation of multiple sclerosis lesions in intensity corrected multispectral MRI," IEEE Trans. Med. Imag., vol. 15. pp. 154–169, Apr. 1996.

[25]. T. Kapur, W. E. L. Grimson, W. M. Wells III, and R. Kikinis, "Segmentation of brain tissue from magnetic resonance images," Med. Imag. Anal., vol. 1, no. 2, 1996.

[26]. Swain,M, Dash S.K, Dash.S and Mohapatra.A (2012), An Approach for iris plant classification using neural network, International journal on Soft Computing, Vol.3,No.1, pp.79.

Dr.K.Baskaran received the B.Tech. Degree in Electronics and Instrumentation Engineering from the Pondicherry Engineering College at Pondicherry University, Puducherry, in 2004, the M.E.degree in Applied Electronics from the Anna University, Chennai, in 2007, and He has completed PhD degree from Annamalai University, Chidambaram in field of Medical Image Processing. He is an Biomedical Engineer and Regional Sales Manager in Gentech Marketing and Distribution Pvt Ltd., New Delhi. and Associate Professor, Department of ECE, Aditya College of Engineering at Madanapalle, AP. He has authored more than 20 publications in international journals and conferences. His research interests include medical image analysis, Bio Signals & Data Acquisition system and VLSI Design.

Dr.R.Malathi is serving as Professor in the department of Instrumentation Engineering and having a working experience of 21 years. She received the B.E.Degree from the Government College Technology in 1990 in the field of Instrumentation and Control Engineering and the M.E.Degree from Madras Institute of Technology in 1992 in the field of Instrumentation Engineering and Ph.D. degree from IIT, Madras in 2009 in the field of Bio Engineering. She received many International awards for her research findings and Best PhD Thesis Award from IIT Madras. She is life time member of many professional bodies. She authored over 80 publications in international journals and conference proceedings, she served has chair for many International Conferences, and being as a reviewer for several international journals. Her research interests include Computational Bio Engineering, Bio Signal and image processing, Bio Sensors and Cardiac electrophysiology.